

# An IceCube-centered Radio-Cherenkov Ultra-high Energy Cosmogenic Neutrino Detector

R. Morse, P. Allison, M. DuVernois, P. Gorham, J. Learned, & G. Varner, *Dept. of Physics and Astronomy, Univ. of Hawaii, Manoa, HI 96822*; D. Besson, *Dept. of Physics, University of Kansas, Lawrence, KS 66045*; A. Karle, F. Halzen, & H. Landsman, *Dept. of Physics, University of Wisconsin, Madison, WI 53703*; J. Beatty, *Dept. of Physics, The Ohio State University, Columbus, OH 43210*; K. Hoffman, *Dept. of Physics, Univ. of Maryland, College Park, MD 20742*; D. Seckel, *Dept. of Physics and Astronomy, Univ. of Delaware, Newark, DE 19716*; D. Cowen, & D. Williams, *Dept. of Physics, Penn State Univ., University Park, PA 16802*; I. Kravchenko, *LNS, Massachusetts Institute of Technology, Cambridge, MA 02139*; P. Chen, *Dept. of Physics, National Taiwan Univ., Taipei 106, Taiwan.*; R. Nichol & A. Connolly, *Dept. Physics & Astronomy, Univ. College London, LONDON WC1E 6BT.*

## I. SUMMARY OF SCIENCE GOALS

We propose here to begin phased development of a low-cost, high-value radio-Cherenkov augmentation to the IceCube detector which will seek the following scientific goals:

1. Extend IceCube energy sensitivity to ExaVolt energies, to yield substantial rates of cosmogenic neutrinos—the so-called “guaranteed” neutrinos.
2. Determine source directions for each neutrino to degree-scale precision, thus identifying directly the sources of the highest energy cosmic rays, which produce the cosmogenic ultra-high energy neutrinos.
3. Co-detect hybrid events with the main IceCube detector, yielding both primary vertex energy via radio-Cherenkov and secondary lepton energy via optical Cherenkov, for complete event calorimetry on a subset of the total neutrino events.

Our proposed system has the potential to significantly enhance the scientific reach of IceCube with regard to total ultra-high energy neutrino event calorimetry, an important and compelling scientific challenge. As we will argue here, a wide-scale radio-Cherenkov [1] detector is a natural and highly complementary addition to IceCube. Recent improvements in the understanding of the radio Cherenkov method [2–5], and its advancing technological maturity have greatly reduced both the risk of such systems and their costs. The time to consider such an augmentation is upon us: once IceCube construction nears completion and the infrastructure and human resources begin to dissipate, the costs for such a system will rise immeasurably.

## II. SCIENTIFIC MOTIVATION

The typical charged-current neutrino-nucleon deep-inelastic scattering event that leads to a detectable secondary muon (or potentially a tau lepton for tau neutrino primaries) in IceCube is  $\nu + N \rightarrow \ell^\pm + X$  where the lepton  $\ell^\pm$  may then propagate for 20-30 km or more before

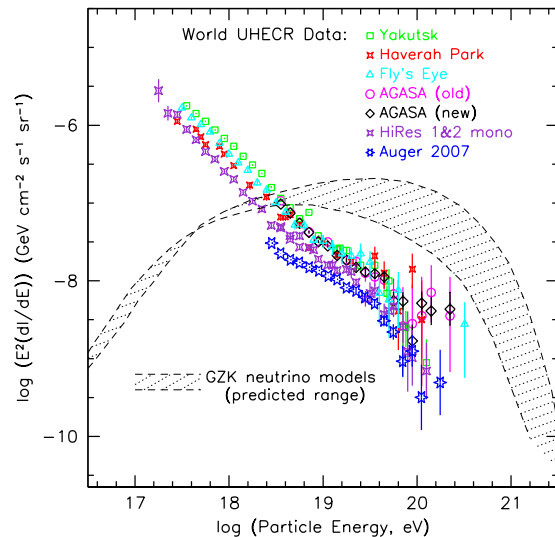


FIG. 1: World ultra-high energy cosmic ray and predicted cosmogenic neutrino spectrum as of early 2007, including data from the Yakutsk [11], Haverah Park [12], the Fly's Eye [16], AGASA [13], HiRes [14], and Auger [15], collaborations. Data points represent differential flux  $dI(E)/dE$ , multiplied by  $E^2$ . Error bars are statistical only. GZK neutrino models are from Protheroe & Johnson [18] and Kalashev et al. [19].

it is detected in the optical Cherenkov array [22]. This potentially long propagation distance leads to an unknown amount of lost energy, and the measurement of lepton energy in an array such as IceCube can thus only provide a lower limit on the energy of the original neutrino. The kinematics of the event is such that the lepton typically carries 75-80% of the primary neutrino energy, with the remainder dumped into a local hadronic cascade initiated by the hadronic debris  $X$  above. This cascade, while initiated by hadrons, rapidly develops into a characteristic  $e^+e^-\gamma$  shower in ice. As has now been shown in a series of recent experiments at SLAC [10], such cascades produce a charge asymmetry as postulated by Askaryan in the early 1960's, and the net negative charge produces strong coherent Cherenkov radio emission, detectable at great distances in a radio-transparent medium such as Antarctic

ice. Thus a suitably stationed array of antennas in a configuration surrounding IceCube on the scale of several km to several tens of km will observe the Cherenkov emission from the primary vertex of the same events that may produce detectable leptons in IceCube. Such a radio array is insensitive to the secondary lepton, but even a relatively coarse array with km-scale spacing between small-number antenna clusters, can coherently detect the strong radio impulses from the cascade vertex. The two methods are thus truly complementary in their physics reach.

One may ask why such a methodology was not adopted early in the design for IceCube. The answer is that the energy of the events that are detectable by a wide-scale radio array is well above the initial design scale for IceCube, intended to go to PeV scales but initially not above this scale. However, since construction of IceCube began, much work has been done on understanding the high-energy reach of the array beyond the original design scale, and it is now evident that IceCube does have significant reach [17] into the range where there is useful overlap between the techniques. In addition, work on understanding the properties of the Askaryan effect and the radiation it produces has proceeded steadily, and we are now in a position to make confident predictions regarding the sensitivity of radio arrays.

This has been facilitated to a large degree by renewed interest in a particular set of neutrino models sometimes called the “guaranteed neutrinos”—those that arise from the interactions of the highest energy cosmic rays with the microwave background radiation throughout the universe [8, 9]. Such cosmogenic neutrinos, as they are also known, are required by all standard model physics that we know of, and their fluxes are tied closely to the parent fluxes of the ultra-high energy cosmic rays which engender them.

Our design approach has been to require that any radio array that would provide hybrid detection with IceCube must be able to detect such neutrinos with confidence in a single year of operation, even at their lowest plausible fluxes. In addition, we expect that the economy of scale for radio technology, which has been greatly enhanced within the last two decades by the explosion in wireless, microwave, and satellite television device development, will lead to an array that is highly affordable on the scale of a small fraction of the costs for IceCube, operating within the scope of an enhancement to the original array. To this end, our choices for the arrays studied have strongly leaned toward giving up spatial and angular resolution in favor of high sensitivity, to maximize the probability for both overall UHE cosmogenic neutrino detection, and hybrid radio/IceCube detections, at minimum cost.

**The Highest Energy Neutrinos.** A proper evaluation of our approach requires an understanding of the distinct nature of the cosmogenic neutrino flux which provides the

basis for our design. Figure 1 shows the ultra-high energy cosmic ray flux as of 2007, with a shaded band indicating the cosmogenic neutrino flux range that results from the interactions of these cosmic rays in intergalactic space. While current uncertainty in the observations of the Greisen-Zatsepin-Kuzmin (GZK) [6, 7] cutoff continue to allow for a relatively wide range of cosmogenic neutrino fluxes, the ongoing measurements of the UHECR fluxes by the Auger Observatory [15], as well as experiments such as ANITA [35], will soon lead to much better constraints on these “guaranteed” neutrino models. Thus we expect a significant narrowing of the allowed range of fluxes in the next several years.

It is important to note that UHE cosmogenic neutrinos peak at energies of order  $10^{18}$  eV, well above the canonical range of IceCube, and in fact even well above the  $\sim 10$  PeV threshold at which radio detection for an embedded or surface ice array becomes practical. Thus, as we will discuss more below, it is possible to design arrays that are much coarser-grained than would be required at the threshold energy for the technique, and to make use of far fewer detectors overall in reaching a given level of sensitivity for the cosmogenic neutrino fluxes. This has important implications for the economics of our studied detectors.

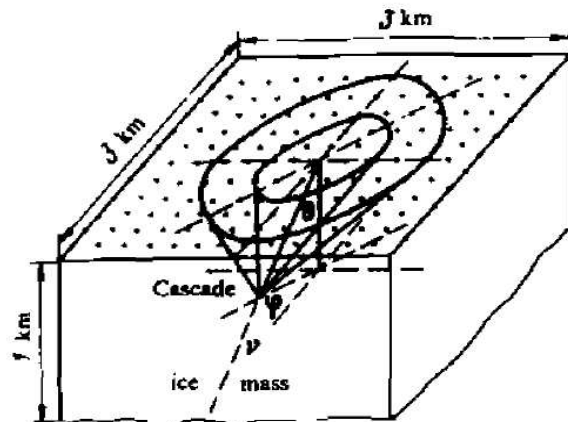


FIG. 2: Original figure from reference [24] in which a surface radio antenna array is used to detect high energy neutrino cascades.

**Radio Detection History.** It is surprising to find that proposals for multi-cubic-km radio Cherenkov detectors in ice are concurrent or perhaps even predate the earliest suggestions that an optical Cherenkov array in ice could engender neutrino astronomy, but that is in fact the case. In the early 1980’s, several Russian investigators began to revisit Askaryan’s suggestions [1] regarding coherent radio detection of high energy particles in dense media such as ice, and in 1984, Gusev and Zheleznykh described an array that utilized this methodology.

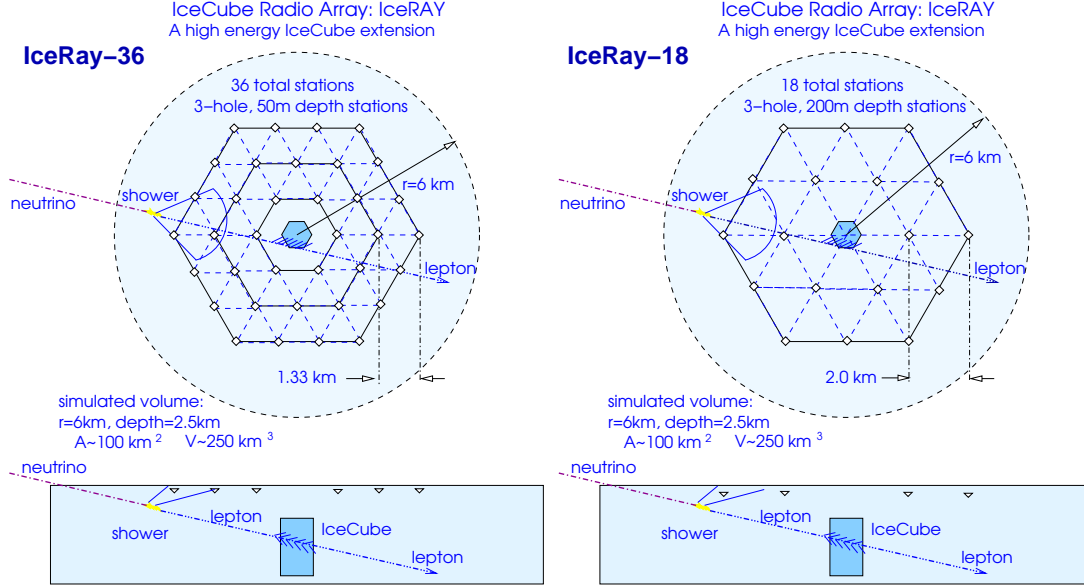


FIG. 3: Left: Baseline 36 station, 50-m depth array, in a plan view (top) and side view (bottom) showing the simulated interaction region around the detector. Right: Alternative 200 m depth, 18 station array.

Figure 2 shows the original figure from the paper by Gusev and Zheleznykh [24] in which a surface radio array with a  $\sim 10 \text{ km}^2$  footprint is proposed to detect of order 10 PeV neutrinos via antennas with grid spacing of several hundred m.

In the later 1980's and early 1990's further investigations were done on the feasibility of the technique, and a landmark paper was published in 1992 in which E. Zas, F. Halzen, and T. Stanev [26] first presented detailed shower simulations which included electrodynamics in a compelling and comprehensive way. This paper gave high credibility to Askaryan's predictions and made the first quantitative parameterization of the radio emission, both in its frequency dependence, and angular spectrum.

Since those results in the early 1990's, the field has grown steadily with the recognition that the relatively high neutrino energy threshold, 10 PeV or more in a reasonably scaled embedded detector in ice, and even higher for other geometries, is well-matched to a number of emerging models for high energy neutrino sources and production mechanisms such as the GZK process. Notable efforts are the RICE [28] array, which continues to pilot the study of embedded detector arrays with a small grid of submerged antennas above the AMANDA detector, the GLUE [29] and FORTE [23] experiments, which set the first limits at extremely high energies above  $10^{20}$  eV, and more recently, the ANITA balloon payload [35], which completed a prototype flight in 2004 [31], and its first full-payload flight in early 2007.

### III. ICERAY PROJECT OVERVIEW

We propose to perform a detailed design study, including development and deployment of prototype hardware, that will enable the construction GZK neutrino detector array covering a physical area of  $\sim 50 \text{ km}^2$  (Fig.3), working in concert with the IceCube detector at the South Pole. The full IceRay will be a discovery-class instrument designed to detect at least 4-8 GZK neutrinos per year based on current conservative models, and would serve as the core for expanding to larger precision-measurement arrays of 300 to 1000  $\text{km}^2$ , capable of detecting at least 30-100 GZK neutrinos per year. The present challenge is to determine the number of individual detectors, their spacing and the depth at which these detectors should be buried in the Antarctic Ice. This depth question is paramount, since deeper detectors sample a greater volume of ice, and thus reduce the number of detectors needed to achieve a desired GZK sensitivity. But deeper detectors also require the drilling of deeper boreholes, which can be expensive and time-consuming. The quest is thus to find the optimum detector spacing-depth ratio that maximizes GZK sensitivity while minimizing the cost

Initial IceRay prototype stations will focus on a wide-scale, shallow detector scheme designed to investigate the radio detection properties from the ice surface down to about 50-80 meter depths, or possibly greater using the much cheaper firn-drill techniques, and to establish background levels several km out from the central part of the South Pole station. This will complement investigations using the IceCube boreholes as part of low-level ongoing

study-phase efforts, which have already taken place under the acronym Askaryan Underice Radio Array (AURA). The AURA prototype efforts have allowed some of the current team to already begin investigation of deeper ice through deployments of radio detectors as elements of IceCube strings over the last several seasons, and these detectors and further ongoing efforts for AURA now already provide a first-order testbed for studies of a deep-ice detector. Although not a direct part of the activities proposed and costed here, we discuss AURA in some detail in a later section, since it provides an important facet of the investigation into the utility of deep antenna deployments, without requiring separate high-cost deep boreholes. Our investigations to date have strongly indicated that deeper detectors are more effective than shallow detectors, but now this is a quantitative question: what is the cost-benefit for deeper vs. shallower arrays, given that shallow detector deployments are easier and less costly than the deep deployments. Understanding these trade-offs is a fundamental question confronting the array designers.

**The Plan.** The ice-depth of the detectors and the spacing between them is of paramount importance, and is one of the primary objectives of this study. The detectors are sensitive to the radio Cherenkov signal emitted when these very high energy GZK neutrinos interact and shower in the ice. Since cold Antarctic ice has an attenuation length greater than 1 km for radio emissions in the 60-1000 GHz range, it is possible to detect neutrino signals from interactions that are kilometers away. The basic geometry is initially assumed to be like IceCube, that is, individual detectors are located at the apices of equilateral triangles, which then are formed up into series of expanding hexagons as is shown in Fig. 3.

We request support for three years, or from March 2008 to March 2011. In the first South Pole season (FY-09) we propose to install a surface listening post, IceRay-0, to determine the strength, and duration of radio emission in the 60-1000 MHz region. This surface listening-post also has SCOARA and the NSF interested in how it might be possible to get a continuous monitoring of the EMI situation at South Pole, that is providing not only frequency usage, but amplitude and duration measurements in a continuously logged fashion. Using the combination of ANITA and IceCube technology this installation of the IceRay surface listening-post should be a straight forward installation.

Also in FY-09 we propose installing IceRay-2, or two sub-surface stations at ice depths of between 50-80 meters, or possibly deeper if the firn-drill techniques allow. These activities would serve as a prototyping of the IceRay-36 array, and give us experience of drilling the holes needed for detector installation. In the second season (FY-10) we would propose installing IceRay-3, or 2 more sub-surface stations of ice depths of 50-100 meters, or deeper if developments in firn-drill technology will allow

such extensions.

In the third season (FY-11) our goal is to start work on the full IceRay array, whatever its form—deep or shallow. This would be engendered by a follow-on proposal submitted to continue the project to its planned full-size. In FY-11 the IceCube work should be ramping down so that a seamless transition from IceCube installation to IceRay installation might be achieved.

**IceRay's Relationship to IceCube.** IceRay's relationship to IceCube will be focused to minimize the cost and manpower levels associated with the proposed IceRay installations. IceRay, working through the Wisconsin group, can be scheduled into the IceCube deployment plan with minimum impact. AURA's prior use of the IceCube boreholes, along with IceRay's proposed use of the firn-drill and the deployment winches are examples of making use of equipment that is already on site because of IceCube's needs. In FY-11, after the successful installation of the IceRay equipment and analysis of the data, we could then, with approval, start the full IceRay installation work. FY-11 is also the season when the IceCube deployment will be ramping down, so the degree of coordination between IceCube and IceRay will be reduced.

**Responsibilities and Oversight.** It will be the primary responsibility of the IceRay effort not to slow down or in anyway impede the normal progress of the IceCube installation. A planning and oversight group consisting of members from both the IceCube and IceRay collaborations will be formed up to provide the necessary oversight. Of course, it is the primary mission of the IceRay effort to work as efficiently as possibly within the IceCube environment.

It will also be the responsibility of IceRay to propose the most effective and cost-efficient detector design. To guarantee that we are receiving and responding to responsible reviews we plan to form up an external review panel that can provide annual reviews of our designs and our progress. Such a committee would be formed up from the people that are in the radio-Cherenkov detection discipline

#### IV. ARRAY DESIGN DRIVERS

The field attenuation length for South Polar ice in the upper km is of order 1.3 km [32] at frequencies in the several hundred MHz regime. In finding the maximum spacing at which a Cherenkov array still has good sensitivity without regard for angular resolution, it is reasonable to adopt distances of order the attenuation length in the medium. If the expected signal is large compared to the threshold of the technique, as is the case for the cosmogenic neutrinos, then even larger spacings can be considered, giving up signal strength for physics reach at the expense of some resolution.

In one prior published study of a combined radio and acoustic detector coincident with IceCube[20], the goals

were somewhat different, and the approach was to build the array initially as part of IceCube itself, making use of the upper portions of the IceCube boreholes and then extending it out to larger radii. Such an array preserved angular resolution and PeV-scale sensitivity while gradually extending its size up to the scale where it could begin to detect cosmogenic neutrinos. Our approach here is quite different; driven by the desire to combine with IceCube on the detection of the “guaranteed” cosmogenic neutrino fluxes, the radio array is designed only to maximize such detection as early as possible, at the lowest cost, and with the highest cross-section possible for hybrid detection with IceCube.

We note parenthetically that acoustic techniques [20] in South Polar ice may well be found to be competitive and complementary to the radio methods for a wide-scale array. It is too early to decide this question, since measurements of acoustic attenuation length and noise levels are at a rudimentary stage, but such methods tend to view portions the solid angle around a neutrino cascade event that are disfavored by radio emission, and acoustic methods could thus prove to fill in the gaps left by radio, at potentially even lower costs than radio methods. We thus keep open the possibility that a widescale array should remain flexible to additional sensor suites should such methods mature in the interim.

With such design choices defined, and based on the physics of the interactions as outlined above, the layout of the necessary array must extend out radially from IceCube far enough to begin covering a significant fraction of the range where neutrino vertices are located. At high energies, this favors lepton events coming from near the horizon for IceCube, since that is the direction with the largest probability for neutrino interactions within the 20-30 km range of the resulting muons. For purposes of this proposal, we have chosen to adopt spacings of 1 to 2 km, and grid which occupies an initial 4 km radius around IceCube. We have explored a range of cases, and we focus on two representative examples which capture the required sensitivity, and span a reasonable portion of the depth-spacing trade-space.

Figure 3 shows the two example full-scale IceRay arrays studied in the most detail here. On the left is a 36-station, 50 m deep version with 1.33 km spacing; and on the right, an array with 2 km spacing, 200 m depth, with 18 total stations. In each case a “station” is required to be able to produce standalone measurements of an event, including location of the vertex and a rough calibration of detected energy. The use of polarization information is also presumed to allow for first-order single-station measures of the event momentum vector. To this end we assume each station to consist of 12 antennas 6 of each polarization, horizontal and vertical. The antennas are assumed to have low directivity gain, equivalent to a dipole, with a

dipole-like beam pattern. Directionality is attained by providing local, several-meter baselines within each station’s array, either through a local-grid-positioning of antennas at the surface, or through use of multiple boreholes (of order 3 with 5-10 m spacing) at each submerged station.

**Choice of frequency.** In choosing a frequency range over which such an array will operate, we begin with the range of frequencies over which ice is transparent: from a practical lower limit of several MHz, where time resolution will already be an issue, and backgrounds potentially prohibitive, to of order 1 GHz, where the attenuation length of ice becomes a problem. Antenna designs will generally limit usable fractional bandwidths to no more than 5:1 for extreme broadband designs, and we therefore assume this as the working bandwidth ratio (5:1 indicates the ratio of the upper frequency to the lower frequency).

An antenna’s effective collecting area  $A_e$  is related to its directivity gain  $G$  (the ratio of  $4\pi$  to the antenna’s main beam solid angle) by the standard equation

$$A_e = \frac{G c^2}{4\pi f^2} \quad (1)$$

where  $f$  is the radio frequency and  $c$  is the speed of light. Since the radiation that arrives at the antenna from an Askaryan radio impulse is often described in terms of its peak field strength  $\vec{\mathcal{E}}_p$  in V/m, the resulting voltage induced at a matched-load receiver attached to an antenna is given by

$$V_{rcv} = \vec{\mathcal{E}}_p \cdot \vec{h}_e / 2$$

where the vector effective height  $\vec{h}_e$  has a magnitude given by

$$h_e = 2\sqrt{\frac{ZA_e}{Z_0}} \quad (2)$$

where  $Z$  is the antenna impedance, assumed matched to the receiver here and  $Z_0 = 377 \Omega$ . The direction of the vector effective height is given by the direction of maximum response to an incident linearly-polarized electric field at a frequency where the antenna is responsive.

Coherent Cherenkov radiation arising from the Askaryan effect has a frequency spectrum for which the incident field strength at the peak of the Cherenkov cone rises linearly with frequency, thus

$$R\mathcal{E}_p \simeq A_0 \frac{E_{shower}}{E_0} f \quad \text{V m}^{-1} \text{ MHz}^{-1} \quad (3)$$

where  $R$  is the distance to the shower from the observation point,  $A_0$  is a medium-dependent scale factor,  $E_{shower}$  is the shower energy, and  $E_0$  a reference energy. This dependence will obtain up to frequencies where loss of coherence due to the size of the shower begins to set in,

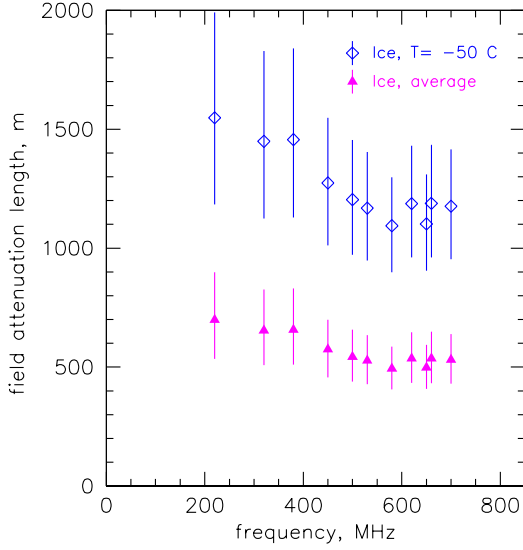


FIG. 4: South pole ice attenuation measurements made in 2004.

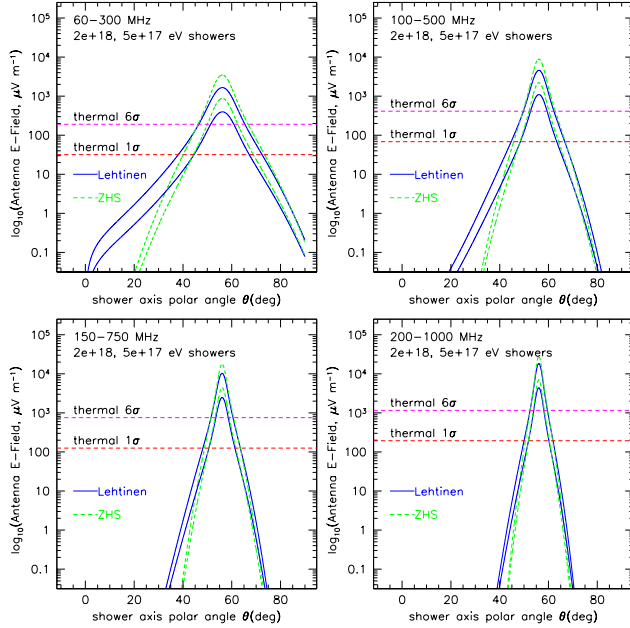


FIG. 5: Angular widths for various frequency ranges and two cascade energies in the heart of the cosmogenic neutrino spectrum. See text for details.

typically near 1 GHz for showers in ice. Thus, solving the equations above, we find the induced signal voltage at the

receiver is given by

$$V_{rcv} = cA_0 \left( \frac{E_{shower}}{E_0} \right) \sqrt{\frac{ZG}{Z_0}} \Delta f \quad (4)$$

which no longer contains any explicit dependence on *frequency*, though a bandwidth dependence remains in the term  $\Delta f$ . If there is also no implicit dependence of the gain  $G$  on frequency, which is often the case with many antennas, then the signal is proportional to bandwidth only, independent of the center frequency.

The system noise is also a consideration, and for a receiver which sees a total system noise (from both the antenna and any intrinsic receiver noise or cable noise)  $T_{sys} = T_{ant} + T_{LNA} + T_{cable} + \dots$ , the RMS induced voltage noise referenced to the input of the receiver is  $V_n = \sqrt{kT_{sys} Z \Delta f}$  where  $k$  is Boltzmann's constant,  $Z$  the receiver impedance, and  $\Delta f$  the bandwidth. Thus the signal-to-noise ratio (SNR) is

$$SNR = \frac{V_{rcv}}{V_n} = cA_0 \left( \frac{E_{shower}}{E_0} \right) \sqrt{\frac{G\Delta f}{kT_{sys}Z_0}} \quad (5)$$

showing that for Askaryan impulse detection, SNR grows with the square-root of bandwidth, but is independent of the center frequency over which this bandwidth is obtained, as long as the antenna gain is approximately independent of frequency. Since it is generally easier to observe larger total bandwidths around higher center frequencies, this appears to favor a higher center frequency for observations, all else being equal.

However, this is not the whole story. Since a neutrino detector depends not only on threshold energy for detection, but also on the total acceptance for events at that energy, we must also consider the dependence of acceptance on radio frequency. There are two terms that contribute to acceptance, one dependent on observable volume of ice, and another on the effective solid angle over which events can arrive and still produce detectable emission.

Effective volume depends generally on the attenuation length of the surrounding ice. Figure 4 shows recent measurements [32] of ice attenuation at the South Pole, based on bottom reflection data. It is evident that there is some frequency dependent increase in losses over the range 200-700 MHz, of order 25-30%. Since the reduction in volume is to first order cubic in the attenuation length, this implies a loss of as much as a factor of 2 in available volume at the two extremes of frequencies here.

The solid-angle for acceptance for any isotropic source, as the cosmogenic neutrinos are expected to be, scales linearly with the solid angle of emission for the Cherenkov cone. The polar angle  $\theta$  of emission around the direction of the shower momentum peaks at the Cherenkov angle.

The angular spectrum of radio Cherenkov emission can be approximated with [23]:

$$F(\theta; f) = \sin \theta e^{-(2\pi cL/f)^2(\cos \theta - 1/n)^2/2} \quad (6)$$

where  $n$  is the index of refraction of the medium, and  $L$  is a parameter describing the characteristic shower length. The resulting solid angle is

$$\Omega(f) = \int_0^\pi F(\theta; f) \sin \theta d\theta d\phi.$$

Clearly, frequency plays an important role in the total solid angle, entering quadratically in the exponential: However, this integral is not analytic, and analysis of the solid angle as a function of frequency is best done numerically.

To understand the behavior of the solid angle terms, we thus refer to actual simulations of the expected signal, based on semi-analytic parameterizations such as that given in equation 6. Figure 5 shows a comparison of the expected signal at a distance of 1.5 km for ice with characteristics of the South Pole. The parameterizations for the radio emission used are those of Zas, Halzen, and Stanev [26] and that given by Lehtinen et al. [23]. The same fractional bandwidth is used in each case, and the noise is scaled assuming an antenna the same directivity gain, constant with frequency, is used for each band considered. There are two important considerations here: first, the strength of the signal on the peak of the Cherenkov cone, which grows with frequency; and second, the width of the Cherenkov cone at the detection threshold, here given as  $6\sigma$  above the thermal noise. The former consideration determines the minimum detectable neutrino energy, while the latter determines the total acceptance by the angular width of the cone where it exceeds detection threshold.

Since the cosmogenic ultra-high energy neutrino spectrum peaks above several times  $10^{17}$  eV, we conclude from this comparison that lower frequencies gain more acceptance and still retain adequate signal-to-noise ratios for detection, as compared to higher frequencies. To put it another way, lowering the energy threshold below the peak of the cosmogenic neutrino flux gains no increase in event rate unless one can preserve the solid angle for acceptance; in this case that does not occur, and a lower frequency array is preferable.

**Refraction effects.** The density of Antarctic deep ice is relatively constant at about  $0.9 \text{ gm cm}^{-3}$ , but near the surface the density rapidly decreases, eventually terminating in the density of the hard-packed snow surface that is common to most of the ice sheet. This has a similar effect on the radio index of refraction and is thus important for relatively shallow embedded arrays such as we consider here. Figure 6 shows this behavior in the index of refraction, which is dependent primarily on the density.

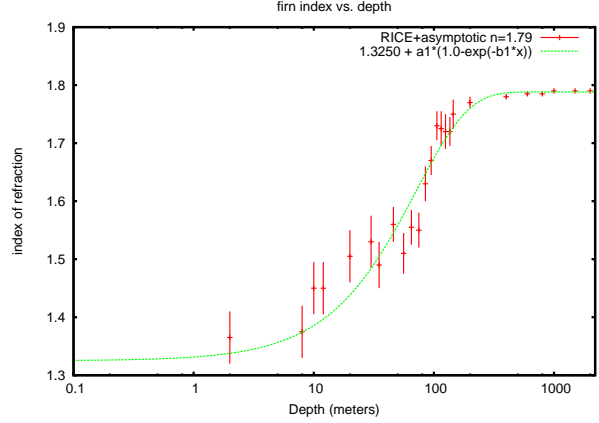


FIG. 6: Index of refraction in firn at South Pole station, based on data from the RICE experiment [28].

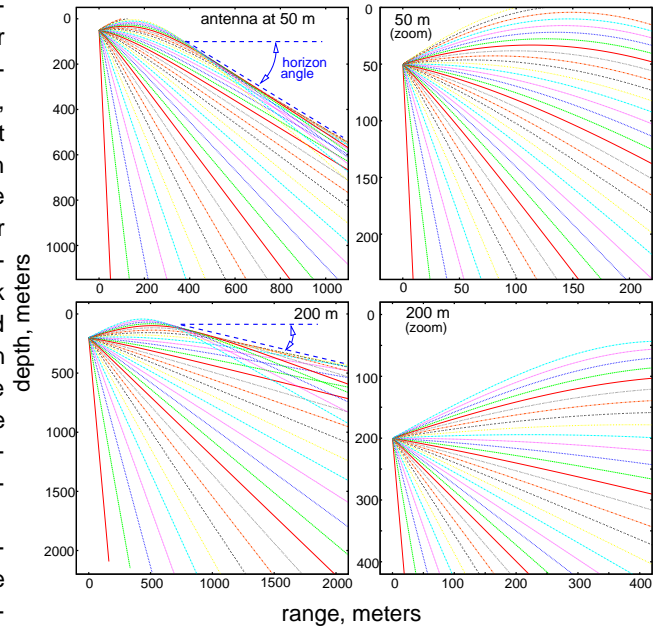


FIG. 7: Example of refraction effects for shallower antenna locations. Both 50 m (upper) and 200 m (lower) deep antenna locations are shown. On the left are the wide-scale ray geometries, showing the terminal horizon angle in each case, and on the right the details of the ray bending in the near zone are shown.

This behavior in the index of refraction must be accounted for in any simulation, and we show here some representative results giving the ray-trace behavior near the surface. This is of particular concern for a relatively shallow subsurface array, and Figure 7 shows a series of rays traced from deep source directions to the near-surface, illustrating the tendency for a near-surface array to see an inverted horizon below the ice, precluding detec-

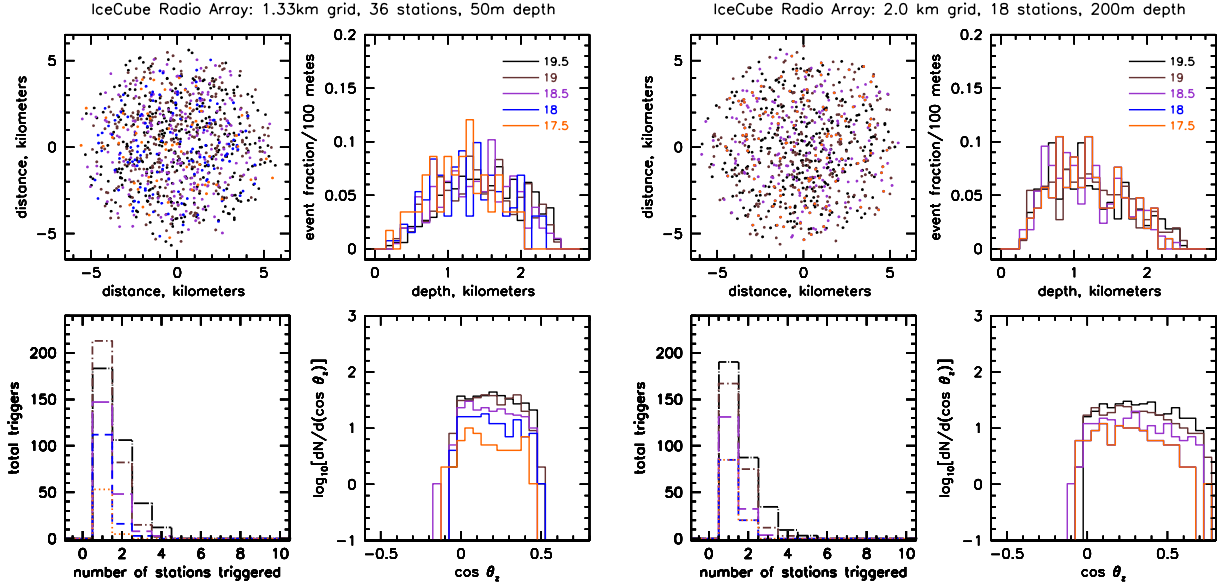


FIG. 8: Histograms of various distributions from the Monte Carlo results for the two configurations studied. Left: distributions for the 36 station array at 50 m depth with 1.33 km spacing; clockwise from upper left: a) the vertex locations in plan view (color coded by energy according to the legend in the next pane to the right); b) the depth distributions of events with energy, with shape governed in part by the refractive horizon; c) the angular distribution of detected neutrino interactions, most events from above the physical horizon, but cut off by the underice refraction at low zenith angles; d) the multi-station hit distribution with energy. Right: similar distributions for the 18-station array with 200 m depth and 2 km spacing with effects of the less restrictive underice refraction horizon evident in the shift of the peaks of the depth distribution, and the wider angular acceptance. However, the coarser station spacing yields fewer multi-station hits.

tion of source above a conical region below the detector. Such concerns limit both the effective volume for a near-surface detector, and the solid angle above the horizon over which events can be seen, and the effect, while significantly less for more deeply submerged antennas, cannot be neglected in either the 50 m or 200 m array depths we studied here.

## V. MONTE CARLO RESULTS

We have studied these arrays with three completely independent Monte Carlo codes (MCCs), and find good agreement with all of them. In addition, the Univ. of Delaware has done MCC studies of some of the specifics of the underice detection, and has independently validated several important aspects of the investigations. The most detailed studies to date were done with the UH Monte Carlo (developed for ANITA and SaLSA) from which most of the plots here are derived, but IceRay-36 and -18 studies have also been done with both the Kansas MCC under the direction of D. Besson, modified from the RICE code, and from the UC London MCC under the direction of A. Connolly, which has been developed both for ANITA project and for studies of the ice-surface array ARIANNA. Thus we have considerable confidence that our basic approach has been validated to the highest degree currently

possible in simulations, and the simulations themselves have been validated with a variety of experimental efforts.

Figure 8 shows results for some standard distributions for both of the studied arrays, as a function of neutrino energy, over a range of energies important to cosmogenic neutrino detection. Detections are allowed up to 2 km beyond the outer perimeter of the arrays in each case, and this additional volume is important in both cases at higher energies, as seen in the upper left panes of each plot. Distributions of detected events (upper right in each set) with depth show the distinct behavior for the 50 m deep array due to the effective “exclusion zone,” or horizon, caused by the firm shadowing of events, whereas the deeper 200 m array shows more uniform range for detection. On the lower right a plot of the angular distribution of events shows the cutoffs imposed by firm shadowing for both arrays, although much less restrictive for the submerged array. Finally, on the lower left the multi-station hit distributions are shown—the denser array has a clear advantage here, and will as a result give a larger fraction of events with high-precision measurements of the event geometry and kinematics.

Figure 9 shows the volumetric acceptance of several of the arrays studied, including a surface-array with 60 sta-

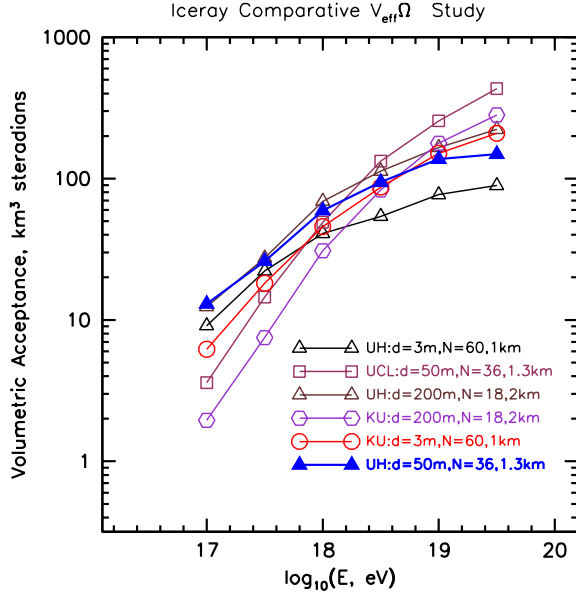


FIG. 9: Volumetric acceptance, in  $\text{km}^3$  steradians, of several arrays studied here, including results from the three independent Monte Carlos within our collaboration: UH indicates Univ. of Hawaii, KU the Univ. of Kansas, and UCL the Univ. College London.

tions, 1 km spacing, and 3 m depth, which was found to be constrained by the losses in the firn refraction, and helps to indicate the importance of getting at least part-way below the firn. Each curve shows the volumetric acceptance, in water-equivalent  $\text{km}^3$  times steradians plotted as a function of energy over the range of interest for cosmogenic neutrinos. IceRay-18 generally gives somewhat higher acceptance than IceRay-36 at the highest energies, but at the cost of slower turn-on at the lowest energies of interest, where it has a smaller net acceptance, attributable to the coarser spacing of this array.

It is evident also that, although the three independent Monte Carlos indicate a generally different energy dependence, and vary widely at the extrema of the energy range, they agree to of order a factor of 2 near  $10^{18}$  eV, the heart of the GZK neutrino spectrum, and as a result give very similar integrated event rates. We stress that these codes evolved and are maintained completely independently, and that the production runs for these results involved no use of any common data other than the detector configuration. It is thus encouraging to see this level of convergence at an early stage, and we assert that we can proceed in our design study with good confidence that the scale of the detector we propose is correct to first order. The IceRay proposal concept is robust and sound, and we can achieve the levels of sensitivity we describe here.

Table I shows the results for the IceRay-36 and IceRay-18 arrays in tabular form, and also approximately factors out the solid angle, to give some additional insight into the differences: the 18-station version gains considerably in solid angle because of its 200 m depth, which reduces the horizon losses under the ice, while the 36 station array makes up for this in the better sampling of the volume that the higher-number-density array affords.

TABLE I: Acceptance and its factors as a function of energy for the two primary example arrays considered here.

$\log_{10}(\text{Neutrino Energy})$	17	17.5	18	18.5	19	19.5
Interaction Length, kmwe	2650	1744	1148	756	498	328
IceRay-36 $V_{eff}\Omega$ ( $\text{km}^3$ sr)	13	26	60	94	137	149
IceRay-36 $\Omega$ (sr)	2.4	2.4	2.1	1.8	1.7	1.6
IceRay-18 $V_{eff}\Omega$ ( $\text{km}^3$ sr)	11.6	38	63	115	137	185
IceRay-18 $\Omega$ (sr)	3	4.4	4.2	4.1	3.8	3.8

TABLE II: Event rates per year for several classes of UHE cosmogenic neutrino models. The lowest two models are in direct conflict with observations, which do not favor a strong iron content for the UHECR; and the next model assumes no evolution of the cosmic ray sources, which is also a scenario that is improbable for known UHECR source candidates.

Cosmogenic neutrino model	36sta/50m events/yr	18sta/200m events/yr
Fe UHECR, std. evolution	0.50	0.60
Fe UHECR strong src. evol.	1.6	1.8
ESS 2001, $\Omega_m = 0.3$ , $\Omega_\Lambda = 0.7$	3.5	4.4
Waxman-Bahcall-based GZK-v flux	4.2	4.8
Protheroe and other standard models	4.2-7.8	5.5-9.1
Strong-source evolution (ESS,others)	12-21	13.8-28
Maximal, saturate all bounds	24-40	32-47

The most important results come after the acceptance has been integrated over various current cosmogenic neutrino models, and the results of such an integration are shown in table II. The lowest two models [30] are in direct conflict with observations [14], which do not favor a strong iron content for the UHECR since models cannot reproduce the observed UHECR spectral endpoint. Such models are detectable on a several-year timescale, but would yield very few hybrid events and are not considered further. The next three “standard model” cosmogenic fluxes give 4-9 events per year. Such events would be dramatic in general, and we expect no irreducible physics background, so detection of even a few events is statistically plausible here. If stronger source evolution obtains, or cosmogenic neutrinos experience other enhancements still allowed by the current limits, these arrays would go beyond detection in a single year, and would begin to provide statistics adequate to develop differential energy spectra on single-year timescales.

Both of the arrays that we have explored in this study have sensitivity for detection of cosmogenic neutrinos on

single-year timescales. We thus have developed the basic outline of a design that can achieve the first two of our science goals. It thus remains still to understand the fraction of such events that will provide hybrid event detection with IceCube.

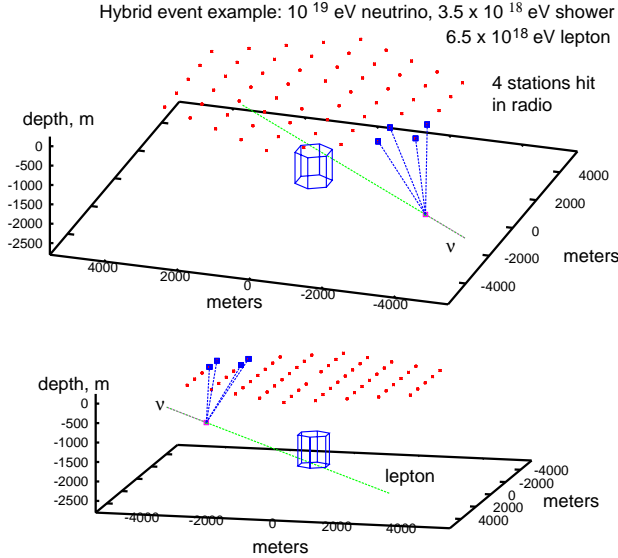


FIG. 10: Example of a hybrid event where the vertex is seen by 4 surface radio detectors and the resulting lepton passes near enough to IceCube to make a detection

### Hybrid Events.

Not all three neutrino flavors, nor all neutrino-initiated showers can yield hybrid IceCube detections. Neutral current events produce no secondary charged lepton, and will comprise about 20% of all events. In the remaining 80% of charged-current interactions, electron neutrinos undergoing yield a secondary high energy electron which interacts very quickly to produce a secondary electromagnetic shower. Muon and tau neutrinos do produce secondary penetrating leptons which can be detectable at IceCube.

At EeV energies in the heart of the cosmogenic neutrino spectrum, the secondary leptons deposit large amounts on energy quasi-continuously along their tracks, and are detectable optically from several hundred meters distance. Secondary EeV muons yield strong electromagnetic subshowers primarily through hard bremsstrahlung and pair production. Secondary tau neutrinos at these energies give their largest secondary showers through photohadronic interactions, and may also produce a strong shower upon their decay, although they typically must fall below 0.1 EeV through energy loss prior to this. in our

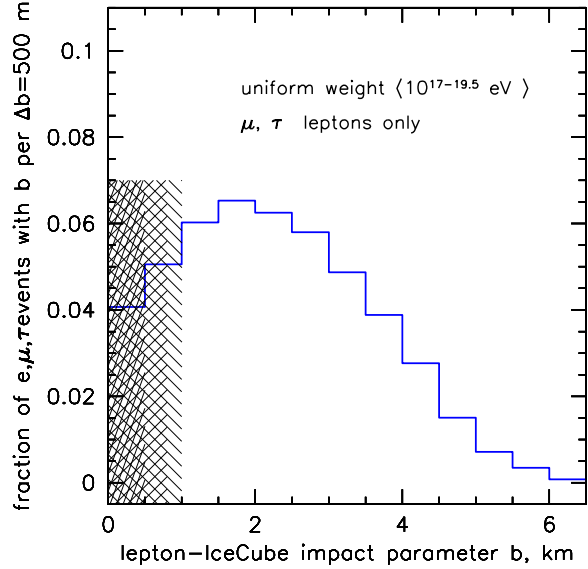


FIG. 11: The distribution of impact parameters relative to the center of IceCube for the outgoing leptons for both muon and tau neutrino events.

simulation we have assumed that all three neutrino flavors are equally mixed, and thus the hybrid event fractions reported here apply to 2/3 of the total events, except at the lowest energies where electron-neutrino events comprise a larger fraction than 1/3 of the total.

TABLE III: Hybrid event rates for the baseline IceCube, and IceCube-plus (1.5 km guard ring), per 10 years of operation, for several classes of UHE cosmogenic neutrino models, assuming the IceRay-36, 50m-deep radio array.

Cosmogenic neutrino model	IceCube 10 yrs	IceCube+ 10 yrs
ESS 2001 $\Omega_m = 0.3, \Omega_\Lambda = 0.7$	3.2	6.4
Waxman-Bahcall-based GZK- $\nu$ flux	3.8	7.6
Protheroe and other standard models	3.8-7.1	5.0-8.2
Strong-source evolution (ESS,others)	10-19	13-25
Maximal fluxes, saturate all bounds	22-36	30-44

An example of the overall event geometry for one example is shown in Figure 10. Here we show an event detected by the surface array in which an incident  $10^{19}$  eV neutrino put 35% of its energy into a shower which was seen by 4 of the surface radio detectors, and the secondary lepton passed just outside the IceCube array with initial energy of  $6.5 \times 10^{18}$  eV. At this energy either a muon or tau lepton is losing of order 0.1 EeV per km of track—this level of emission would produce a huge signal at IceCube, even with an impact parameter several hundred meters distance outside the array.

In Figure 11 we quantify the hybrid event detection fractions for the IceRay-36 array, indicating the distribution of all neutrino events vs. their impact parameter  $b$  for 500 m increments, using a graded hatching to denote the regions over which there is a direct detection within the fiducial volume of the IceCube detector, or a detection within a 500 m annular region around the array, as expected for these very high energy (and thus very bright) leptons. We have included electron neutrino events and neutral current events in the total count, even though they do not produce an outgoing long-range lepton, so that the hybrid fractions are with respect to total neutrino events, not just charged-current muon or tau neutrino events.

For the standard IceCube geometry, the total hybrid event fraction is of order 10% in these two regions. Recent studies of “guard-ring” extensions to IceCube [17] have shown the utility of one or more outer rings of strings 500-1000m outside the standard array. If we assume a single ring at a radius of 1 km from the center of IceCube, with itself an additional 500 m of reach for secondary lepton detection, the hybrid fraction extends to 15% of all neutrino events, and a 1.5 km guard ring could yield a hybrid fraction reaching 20%.

Table III gives the resulting total hybrid events expected for the IceRay-36 detector, for two different IceCube configurations, the baseline design, and one that includes a 1.5 km guard ring, known as IceCube-plus. The totals are for ten years of operation, and although they are relatively small totals, they will represent the first set of UHE neutrino events where the complete event topology can be constrained, and calorimetric information can be extracted. In addition, these events should be free of any known physics backgrounds.

Further enhancement of the hybrid subsample can be achieved using sub-threshold cross-triggering techniques, whereby events detected in either IceCube or the radio array would provide a trigger to the other array, allowing the data stream to be searched for contemporaneous signals that might not have been otherwise detectable. For example, IceCube can only observe events that arrive from above the horizon if their energies are very high, far above the atmospheric muon background. However, an apparent atmospheric muon event that was coincident with a radio event with the right geometry could be promoted into the hybrid event subsample. We propose here to quantify the detector requirements to take advantage of such possibilities.

We have also investigated the converse of the IceRay→IceCube hybrid detection scheme we detail above: that is, what fraction of GZK neutrino events detected by IceCube will also be seen by the radio array? For this we estimate a minimum of between 30-50%, but if a core AURA-type array is included within the IceCube central array, then this fraction will grow to of order 100%.

There is thus a strong argument from the point-of-view of hybrid events for continuing the AURA efforts.

## VI. THE ICERAY-36 DETECTOR

The IceRay-36 detector, which we have currently adopted in preference to the 18-station, 200 m deep detector, consists of 36 stations buried 50-80 meters deep in the ice, based on current or projected firn-drill capability. The basic geometry consists of 1.3 km equilateral triangles which form a series of three concentric hexagons with IceCube in their center. While we have adopted the 50 m depth version of IceRay as the baseline, we propose to study the cost-benefit of deeper detectors. Ray-tracing studies do show a steady improvement fiducial volume in with increasing depth up to about 400-500 meters, however drilling cost certainly do increase. One can compensate for the reduced volume sampled by shallow depth detectors by employing more of them. The present IceRay schemes also calls for three boreholes per detector station, most probably arranged on the apices of an 8-10 meter equilateral triangle. Such an arrangement will provide not only multi-fold coincidence information, but timing-phase information will allow directions to be determine to 1-2 degrees or better depending on signal power.

**Design.** Each detection station consists of an array of 12-16 wideband antennas, each instrumented with band-pass filters and amplifiers adjacent to each antenna down hole. Considerable effort has already gone into antenna design and optimization and this topic will certainly be further addressed as part of our study, although for brevity we do not detail these here. The amplified RF signal is transmitted via coaxial cable to trigger and digitization electronics located on the surface. Amplification of approximately 76 dB is needed to boost the signal from thermal noise levels to an amplitude large enough for direct triggering and digitization. The trigger scheme [34] has been successfully flown on the ANITA payload [35]. Each detector station is connected via fiber optic and a number of station inter-trigger and readout topologies have been considered, one such study has been published [36]. The first year prototype has been based upon the LABRADOR3 ASIC [37], used by both ANITA and AURA. However, for being able to store an entire array transit time for sub-threshold event reconstruction, a next generation trip based upon the BLAB chip [38] will be used. First generation prototypes are 64k samples deep, permitting 64us of buffering at 1GSa/s. Local station triggers are formed based upon temporal and spatial coincidences in the antenna signals and broadcast to the central recording station to force complete array readout.

**Construction.** Antennas will be designed, constructed, and tested at both Kansas and Hawaii. Both institutions have had extensive experience in this area with their pursuits of RICE and ANITA. Both institutions have Anechoic

Chambers and equipment required to completely characterize antennas, such as measuring complex impedance and VSWR in both the frequency and time-domain. For short-pulse work, the time-domain is the proper domain in which to characterize the antennas. Since the antennas are physically small protecting them is not a major problem. The antenna arrangement will be back-filled with snow, so that in time, the antennas will see an almost uniform environment of snow and a constant index of refraction.

The signals detected by the antennas are fed to the LNAs and then run to the surface via coaxial cables to a data collection box (DCBs) on the surface. In addition, this shielded DCB accepts the power to run all the devices from the station DC power supply and cable system. The DCBs also provides additional amplification of each of the antenna channels. The various antenna signals are then routed to discriminators to determine that we have a signal of interest, and if they trigger, the signals are then run to the BLAB digitizers, where their full time-amplitude development is digitized, and the data is routed via the power-signal cable to the Central DAQ in the ICL. We are also going to investigate possibly sending the data over a fiber-optic line.

**IceRay Integration.** Present planning calls for IceRay components to be shipped to Wisconsin's Physical Sciences Lab (PSL) for final testing and integration. This is, and has been, standard procedure for all IceCube equipment and AURA equipment that will be installed at South Pole. Specifically for IceRay, we plan to use PSL's 24 x 25 ft anechoic chamber which is capable of being cooled to -50C to provide test conditions that are quite similar to austral winter situations at South Pole, where the ice temperatures a few meters below the surface generally average about -50C. We plan to conduct full system tests, from antennas to DAQ read-outs before we would certify the system as ready for shipment. PSL has all of the standard electronic equipment needed to conduct most of these tests, and has the technical people needed to conduct them.

**Ice Drilling and Deployments.** Each station requires three holes 50-80 meter deep, and 60 cm in diameter to accommodate the antennas. Present plans are to use the IceCube "firn" drill, a "hotpoint" style drill that specializes in drilling through the firn: that porous ice that makes up the first 50-70 meters of low-density ice just below the surface. We also will investigate what is needed to extend the reach of the firn drill to depths of 100-200 meters. The present IceCube firn-drill uses about 150 kW and can drill at a rate of about 4 m/hour. The whole setup is about 24 ft long by 8 ft wide. It circulates about 15-20 gpm of hot fluid (60-40 mix of propylene glycol and water) to the head at about 75 deg. C. (returning 15 to 30 C cooler depending on drill rate). The heaters come on and off as needed to

maintain the fluid tank at 75C. The total available power is 150 kW but we rarely used it all. We usually had about 3 or 4 heaters on (@ 30kW) at a time so we probably averaged about 100 kW for most of the hole. We drilled about 6 meters/minute near the top of the hole and at about 3 meters/minute at the bottom (around 38-40 m deep). The system would start to slow down somewhat below where we start to get in to pooling water. This could slow down drill progress. That remains to be seen but we did find we were drilling with all 5 heaters running more of the time.

**Power and Signal Transport.** Each detector station will consume of order 50 watts of power. The present plan is to run both the power and the signals over copper lines, though we will be looking into a combo-cable that carries both power and fiber optics. This design will require an optimization scheme that depends on the total number of detectors planned. For example, the designs as to wire-sizes and wire paths might be quite different for IceRay-36 as opposed to an IceRay-300 design. The present cable design has been supplied by Ericsson, who also makes the IceCube cables. It consists of three twisted-quads or 12 0.9mm wires (#19 AWG). Two of the quads carry 100 watts of 120 VDC power, while the third quad carries the signals from the detector location approximately 2 km to the ICL. The voltage drop is about 25 volts over 2 km, so it represent about a 25% power-loss in the cables. It is expected that we will supply about 125 VDC at the ICL to obtain about 100 volts and 1 amp at the detector to supply power to the various DC to DC converters. The signal transmission over 2 km is not that challenging at the expected data bandwidths required. This is quite similar to the IceCube data transfer requirements from 2.4 km depths, using the same type of cables.

**Control & Data Handling.** The IceCube infrastructure is used for communication, control, timing, data handling and data transfer to the northern hemisphere. Once a multiple bands and antenna triggers occurs, the digitized waveforms are read from all the antennas, packed and sent to a special designated host machine located in the IceCube Counting house on a special crate. A surface cable from the surface junction box runs to the central counting house. The South Pole host machines (hubs) are standard industrial Single Board Computers. The communication is done through a customized PCI cards developed for IceCube (DOM Readout card). The hub is also equipped with a special service board distributing the GPS time string to all PCI cards. Each hub is customized with +48 Volt and -48 Volt switching regulated AC-DC single output power supplies, to supply 96 Volts to the main boards. Each DOR card can connect to two power and communication wire pairs. For IceCube, they were used to connect two adjacent DOMs on a string. We will use one of the wires to connect to the main board, and the other to supply additional power to the RF amplifiers us-

ing an external power supply. Timing with an accuracy of a few ns is achieved by using the RAPCAL method as used by IceCube. Offline processing looking for time coincided between several stations and with IceCube, will further filter the data.

**Analysis—Pass One** Early verification analysis include vertex reconstruction using an in ice RF source or a surface transmitter. This will verify the expected time resolution, waveform reconstruction and vertexing. Such a measurements will also allow Linearity and Amplitude calibration. Ambient and transient background measurements will be used to study the EMI background around the South Pole, and the environment suitability for RF detection. Since the detector is buried in shallow snow, and not in water (like IceCube) data can be taken as soon as the detector is plugged in. Not only will this allow EMI measurements during the summer period where the South Pole station is busy, it will also allow trouble shooting of the detector and cables before season ends, and experts are still on ice. Events times will be compared to IceCube's trigger times looking for coincidental events in both directions: looking for RF event when strong IceCube triggers occurred, and also looking for IceCube events when strong RF events were detected (This will require some tuning of the IceCube trigger scheme, to keep this data from being filtered out).

### Linked Assets: AURA

RICE (the Radio Ice Cerenkov Experiment) was the first array in the Antarctic to employ the Askaryan effect in the search for neutrinos and other high energy phenomena. Since it began operations, RICE has mapped out the South Pole RF noise environment, studied the RF properties of the cold South Polar ice, and developed techniques for radio analysis, eventually setting limits on low scale gravity and other high-energy phenomena. Following on the success of RICE, which was largely deployed parasitically to the AMANDA installation, the AURA collaboration was formed to exploit the unique opportunity created by IceCube operations to deploy radio antennas over a larger footprint and at greater depths. Further, the electronics and infrastructure developed by IceCube to provide power, time synchronization, and data readout across large distances, along with radio specific hardware developed for ANITA, have been used as a spring board to quickly develop radio instrumentation that could be scaled up to a large glacial array for GZK neutrino studies.

AURA currently consists of a set of radio detectors buried between 250-1400 meters in the Antarctic ice. These detectors are designed to measure the radio characteristics of the deep ice. Selected IceCube boreholes have radio receivers installed in them to measure the radio spectrum from about 200-1000 MHz. In the austral summer of 2006-2007, the first AURA instrumentation was

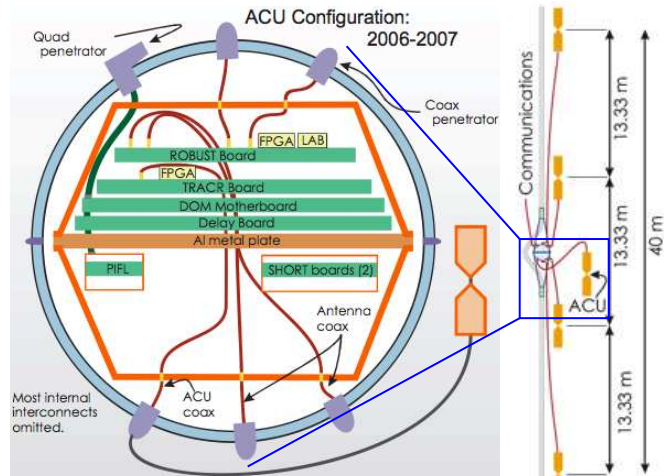


FIG. 12: Left: A schematic of the DRM. Right: its location along an IceCube string.

deployed: two clusters consisting of four receivers and one transmitter, and one cluster with a transmitter only. A schematic of a cluster is shown in Figure 12. The electronics which provide the power, data acquisition, trigger logic and communications are located inside of an IceCube pressure vessel, so that the mechanical mounting and connection of the digital radio module (DRM) could proceed exactly as it does for IceCube digital optical modules, with zero impact on IceCube operations. Present plans call for installing three shallow detectors (250 m depth), and one deep detector (1400 m) in January 2008.

A schematic of the DRM is shown on the right in Figure 12. It holds the TRACR board (Trigger Reduction And Communication for RICE) that controls the calibration signal and the high triggering level, the SHORT board (SURF High Occupancy RF Trigger) that provides frequency banding of the trigger source, the ROBUST card (Read Out Board UHF Sampling and Trigger) that provides band trigger development, high speed digitization and second level trigger discrimination, the LABRADOR (Large Analog Bandwidth Recorder And Digitizer with Ordered Readout) digitization chip, the PIFL supplies the power, and a Motherboard that controls the communication and timing. The sampling speed is 2 GSPS, with a 1.3 GHz bandwidth and 256 ns buffer depth. The simple RICE-style dipole antennas have been used. Located near each antenna are pressure vessels containing front end electronics for amplification and filtering. The digitized data is sent to the surface using the IceCube in-ice and surface cables where it is being processed and analyzed.

The DRM with the single transmitter and one of the transmitter-receiver clusters were deployed in holes drilled 500m apart at a depth of 1450 m with unused connectors in the IceCube cable. This allows a survey of the noise environment in the deep ice, as well as studies of the ef-

fects of the proximity of the IceCube DOMs. The remaining receiver-transmitter cluster was installed at a depth of 250m in a hole near the existing RICE array to allow cross calibration of the two instruments. Since February 2007, when the clusters were first frozen in, they have been operated in both self trigger and forced trigger mode, and to date, a large quantity of data has been transmitted north for analysis. The data being taken consists of ambient and transient background studies, calibration runs using the AURA transmitter and the in-ice RICE transmitters. The first unambiguous confirmation of our ability to receive and digitize radio signals was achieved shortly after deployment with a series of special calibration runs using the RICE continuous waveform transmitter. The effect of IceCube electronics has been studied using the deep transmitter cluster by taking special runs with IceCube turned on and off.

This AURA work has been and will continue to be beneficial and complementary to IceRay in our efforts to learn just how deep in the ice we have to locate the detectors in order to develop a credible GZK neutrino array. Deep access is provided as a result of the IceCube string deployments, and from the point-of-view of the current IceRay proposal, the utilization of these resources with minimal impact on IceCube provides important added-value to the decision process for a wide-scale radio array.

## VII. PRIOR & ONGOING NSF SUPPORT RESULTS

The proposal members have contributed to a variety of successful NSF supported research programs, including AMANDA, Auger, IceCube, and RICE.

**AMANDA (Antarctic Muon And Neutrino Detector Array).** UW (including R. Morse, AMANDA Principal Investigator, now at UH) has been the lead US institution in the AMANDA collaboration. AMANDA pioneered the use of an array of photo-multiplier tubes in deep clear polar ice to gather Cerenkov light from neutrino generated muons. AMANDA served as a testbed for deployment, DAQ, calibration and analysis techniques that have been vital for development of the IceCube detector. Late in life AMANDA is operating as a high density low threshold component of IceCube. Data from earlier years is producing a steady output of scientific papers on virtually all subjects of high energy neutrino Astronomy, from atmospheric neutrinos to constraints on AGN models with neutrino energies above a PeV.

**Auger.** J. Beatty (OSU) is a leading member of the Auger collaboration, and serves as Task Leader for the Auger Surface Detector Electronics. The OSU group is involved in work on data acquisition, calibration, and data analysis focusing on the surface detector. The southern Auger detector is nearly complete, and results concerning the spectrum, anisotropy, and composition of the highest

energy cosmic rays are being released.

**IceCube.** Members of this IceRay/AURA proposal from UW, UMd, UD, and KU are all collaborating members of the IceCube collaboration. This includes NSF support for the construction of IceCube managed through UW and disbursed to US collaborators, as well as 'Physics analysis' grants to the individual institutions. The main component of IceCube is a 1 km<sup>3</sup> neutrino detector, deployed at a mean depth of 2 km at South Pole. The detector consists of an array of PMTs for detecting optical Cerenkov signals - ultimately due to neutrino interactions in deep ice, or in bedrock below the detector. The detector is approximately 1/4 finished. It has an operational live time of better than 95%, and is transmitting ~ 30 GB of filtered data per day to the northern hemisphere. Using data from the first year of physics operation (~ 12% of full array), the collaboration has already produced its first scientific paper on the atmospheric neutrino flux. The experiment also includes IceTop, an array of frozen water tanks, reminiscent of Auger tanks, for detecting cosmic ray induced air showers. In coincidence with the in-ice detector, such events are useful for cosmic ray science, calibration, and vetoing a background of large cosmic ray events which may masquerade as UHE neutrino events in and near the deep detector.

**RICE (Radio Ice Cerenkov Experiment).** D. Besson (KU) is the PI of the RICE experiment. D. Seckel (UD) and I. Kravchenko (MIT) have been collaboration members since its inception in 1995. RICE is a prototype for an englacial neutrino detector utilizing the Askaryan radio technique. RICE has deployed over 20 receivers in the Antarctic ice at South Pole and has collected physics quality data since 2000. RICE data is responsible for the strongest limit on UHE neutrino fluxes in the energy range of 10<sup>17</sup> – 10<sup>18</sup> eV. RICE data has been used to place limits on neutrino nucleon cross-sections in low scale gravity models, the flux of ultra relativistic magnetic monopoles, and the flux of UHE neutrinos from gamma ray bursts.

**ANITA (Antarctic Impulsive Transient Antenna).** While ANITA does not receive direct NSF support, it does receive substantial indirect support through NSF's strong support for the NASA Long Duration Balloon (LDB) Program. Collaborators P. Gorham (PI for ANITA), G. Varner, M. Duvernois, P. Allison, J. Learned, P. Chen, R. Nichol, and A. Connolly have all played important roles in bringing ANITA to the forefront of current UHE neutrino detectors. Without NSF support for LDB and the infrastructure necessary to sustain it, ANITA and similar projects would not be possible.

## VIII. BROADER IMPACTS

As IceRay is intended as an augmentation to IceCube capabilities, we propose to augment IceCube's Education and Public Outreach (EPO) programs with material and

activities that will widen the understanding that Cherenkov radiation, the electromagnetic analog to the more familiar acoustic shock-wave, can have effects across the whole electromagnetic spectrum, including radio. The huge increase in public consumption of radio and wireless-based devices—cell-phones, networks, radio-frequency identification tags, wireless car locks and toll-roads creates an excellent opportunity for public impact as we incorporate the IceRay/AURA methodology into existing IceCube EPO venues. These augmentations are essentially no-cost extensions since the EPO activities are ongoing and can admit new curricular elements at any time.

The IceCube EPO program at the UW Madison has focused on three main areas: providing quality K - 12 teacher professional development, and producing new inquiry-based learning materials that showcase ongoing research; increasing the diversity of the science and technology workforce by partnering with minority institutions and programs that serve underrepresented groups; and enhancing the general public appreciation and understanding of science through informal learning opportunities, including broadcast media and museums. These efforts have been supported by the University of Wisconsin since 2001, and we propose to expand the curriculum with a distinct radio component.

In addition to IceCube's formal EPO program, many efforts to share the excitement of science with students and the public at-large take place at the institutional level as well. Kara Hoffman frequently visits local high schools to talk to students about her life as a scientist and Polar traveler. Within the last year, Dave Besson at the University of Kansas has been giving classes to senior citizens on the subject of astrophysics, with a particular emphasis on his own experience with RICE and AURA. These classes are typically attended by ~50 persons from the Lawrence-Topeka-Kansas City area.

The primary science mission of this proposal lends itself to active undergraduate involvement. RICE has benefited from the efforts of previous physics majors – seven KU undergrads, including Adrienne Juett (Goldwater Scholar, 1998, and MIT, Ph.D., 2005), Dave Schmitz (Goldwater Scholar, 2001, now finishing his Ph.D. at Columbia), Josh Meyers (Goldwater Scholar, 2003, now a grad student with the Perlmutter group at LBL), and Hannah Swift (Goldwater Scholar, 2005, also a grad student with the Perlmutter group at LBL) performed initial work on data analysis and both the attenuation length and index-of-refraction measurements at the South Pole. Current undergrad, and Rhodes Scholar nominee Daniel Hogan is currently finishing an analysis of the sensitivity of RICE to monopoles. The University of Maryland has also involved three undergraduate physics majors to produce simulations to determine the optimal placement of the AURA hardware. We expect to continue this heavy reliance on undergraduates

as the radio effort moves forward in the future.

Several of our institutions also have formal partnerships with local high school teachers as well. The OSU group is working with teacher Doug Forrest at Pickerington North High School in suburban Columbus to incorporate simple cosmic ray experiments into the honors physics high school curriculum. They helped him secure \$11,000 form a local educational foundation for laboratory equipment, and are working with him to design appropriate experiments and educational materials and conduct classroom visits from time to time. We propose that additional radio-based curricular materials will be integrated into this program, and we will seek further funds to adapt a modest radio-detector extension to the current systems.

Both the University of Maryland and the University of Hawaii are heavily involved in the QuarkNet program. Through UH's QuarkNet program, established in 2003, Gorham, Varner, and Learned have been actively involved in developing cosmic ray detectors for classroom use. Morse will take on a contributing role for the UH Quarknet efforts, providing seminar and mentoring contributions to the local Quarknet curriculum. The UH Quarknet program involves both teachers and students from underserved outer-island districts, and a radio-based augmentation to this will have accordingly greater impact. W

UM's QuarkNet chapter was established in 2002, and since her arrival at UM in 2004, Hoffman has been the main organizer and mentor for this group. In the past summer, she ran her third summer teacher institute, and she has been instrumental in increasing participation from ethnically diverse communities. She has also helped secure cosmic ray detectors for several of the teachers she mentors.

- 
- [1] G. A. Askaryan, 1962, JETP 14, 441; 1965, JETP 21, 658.
- [2] P. W. Gorham, D. P. Saltzberg, P. Schoessow, *et al.*, Phys. Rev. E. **62**, 8590 (2000).
- [3] D. Saltzberg, P. Gorham, D. Walz, *et al.* Phys. Rev. Lett., **86**, 2802 (2001).
- [4] P. W. Gorham, D. Saltzberg, R. C. Field, *et al.*, Phys. Rev. D 72, 023002 (2005).
- [5] P. Miočinović, R. C. Field, P. W. Gorham, *et al.*, Phys. Rev. D 74, 043002 (2006).
- [6] K. Greisen, "End To The Cosmic Ray Spectrum?," Phys. Rev. Lett. **16**, 748 (1966).
- [7] G. T. Zatsepin and V. A. Kuzmin, "Upper Limit Of The Spectrum Of Cosmic Rays," JETP Lett. **4**, 78 (1966) [Pisma Zh. Eksp. Teor. Fiz. **4**, 114 (1966)].
- [8] V. S. Berezinsky and G. T. Zatsepin, Phys. Lett. B 28, 423 (1969)
- [9] R. Engel, D. Seckel, and T. Stanev, Phys. Rev. D 64, 093010 (2001).
- [10] P. W. Gorham, *et al.*, [ANITA Collaboration], "Observations of the Askaryan Effect in Ice," (2007), Phys. Rev. Lett. in press; arXiv:hep-ex/0611008.
- [11] A.V.Glushkov *et al.*, Astropart. Phys. 4 (1995) 15.
- [12] M.A. Lawrence, R.J.O. Reid, A.A. Watson. J. Phys. G. 17 (1991) 733.
- [13] S.Yoshida *et al.*, Astropart. Phys. 3 (1995) 105; also Shigeru Yoshida, Hongyue Dai, (astro-ph/9802294). Journal of Physics G 24 (1998) 905.
- [14] R. U. Abbasi, *et al.*, The HiRes Collaboration, (2007) submitted to Phys. Rev. Lett., astro-ph/0703099.
- [15] M. Roth, for the Auger Collaboration, "Measurement of the UHECR energy spectrum using data from the Surface Detector of the Pierre Auger Observatory," Contribution to the 30th International Cosmic Ray Conference, Merida, Mexico, <http://arxiv.org/abs/0706.2096>, 2007.
- [16] D.J.Bird *et al.*, Astrophys. J. 441 (1995) 144. J.W.Elbert, P.Sommers, Astrophys. J. 441 (1995) 151; Baltrusaitas, R.M., Cassidy, G.L., Elbert, J.W., *et al.*, Phys. Rev. D **31**, 2192 (1985).
- [17] F. Halzen, and D. Hooper, JCAP 0401 (2004) 002; astro-ph/0310152.
- [18] R. J. Protheroe & P. A. Johnson, Astropart. Phys. 4, 253 (1996).
- [19] O. E. Kalashev, V. A. Kuzmin, D. V. Semikoz and G. Sigl, "Ultra-high energy neutrino fluxes and their constraints," Phys. Rev. D **66**, 063004 (2002).
- [20] D. Besson, S. Boeser, R. Nahnauer, P.B. Price, and J. A. Vandenbroucke, for the IceCube Collaboration, 29th International Cosmic Ray Conference, Pune, India (2005) 00, 101.
- [21] The AMANDA Collaboration: J. Ahrens, *et al.*, Nucl. Instrum. Meth. A524 (2004) 169.
- [22] The IceCube Collaboration: M. Ackermann *et al.*, Nucl. Instrum. Meth. A556 (2006) 169.
- [23] N. Lehtinen, P. Gorham, A. Jacobson, & R. Roussel-Dupré, Phys. Rev. D 69 (2004) 013008; astro-ph/030965.
- [24] G. A. Gusev, I. M. Zheleznykh, "On the possibility of detection of neutrinos and muons on the basis of radio radiation of cascades in natural dielectric media (antarctic ice sheet and so forth)," SOV PHYS USPEKHI, 1984, 27 (7), 550-552.
- [25] M. A. Markov, I. M. Zheleznykh, Nucl. Instr. Meth. A 248 (1986) 242.
- [26] E. Zas, F. Halzen, & T. Stanev, 1992, Phys Rev D 45, 362.
- [27] I. M. Zheleznykh, 1988, Proc. Neutrino '88, 528; R. D. Dagkesamanskii, & I. M. Zheleznykh, 1989, JETP 50, 233.
- [28] I. Kravchenko *et al.*, Astropart.Phys. 20 195-213 (2003).
- [29] P. W. Gorham, C. L. Hebert, K. M. Liewer, C. J. Naudet, D. Saltzberg, D. Williams, Phys. Rev. Lett. 93 (2004) 041101.
- [30] M. Ave, N. Busca, A. V. Olinto, A. A. Watson, T. Yamamoto, Astropart. Phys. 23 (2005) 19.
- [31] The ANITA Collaboration: S. W. Barwick *et al.*, Phys. Rev. Lett. 96 (2006) 171101.
- [32] S. Barwick, D. Besson, P. Gorham, D. Saltzberg, J. Glaciol. 51 (2005) 231.
- [33] J. Alvarez-Muñiz & E. Zas, 1997, Phys. Lett. B, 411, 218.
- [34] G. Varner, "The Modern FPGA as Discriminator, TDC and ADC," Journal of Instrumentation, Volume 1, P07001 (2006).
- [35] The ANITA Collaboration, presented by G. Varner, "Detection of Ultra High Energy Neutrinos via Coherent Radio Emission," Presented at 9th International Symposium on Detector Development for Particle, Astroparticle and Synchrotron Radiation Experiments (SNIC 2006), Menlo Park, California, 3-6 April 2006, SLAC-PUB-11872, 6pp. May 2006.
- [36] G. Varner *et al.*, "A Giga-bit Ethernet Instrument for SaISA Experiment Readout," Nucl. Instr. Meth. A554 (2005) 437-443.
- [37] G. Varner *et al.*, "Development of a Low-Power Multi-GSa/s TranThe Large Analog Bandwidth Recorder And Digitizer with Ordered Readout (LABRADOR) ASIC," arXiv:physics/0509023v2, accepted for publication by Nucl. Instr. Meth. A Sept. 2007 (in press).
- [38] G. Varner and L. Ruckman, "The Buffered LABRADOR ASIC version 1 (BLAB1)," submitted to Nucl. Instr. Meth. A; initial test results presented SLAC Advanced Instrumentation Seminar, July 11, 2007. [www-group.slac.stanford.edu/ais/](http://www-group.slac.stanford.edu/ais/)

## Budget Justification

**Scope and Phasing of the IceRay Task.** IceRay is scheduled as a three-year multi-university investigation. In the first year season at South Pole (FY-09) we plan to install two remote radio-detectors in proximity to the IceCube detector. These detectors will make almost exclusive use of ANITA technology so that little R&D work is required beyond making them deployable in the deep Antarctic ice. Getting two detectors into the ice is important since it will allow us to study radio correlations between detectors as well as correlations with the IceCube detector.

In the second season at South Pole (FY-10), we plan to install two more radio-detectors near IceCube. These four detectors will yield more detailed information on the correlations between detectors, trigger formation schemes (using electronic pulses), radio propagation through the ice as well as possible IceCube-radio correlations (so-called reverse triggers)

In the third year of the proposal we plan to concentrate fully on the data analysis and the development of more detailed simulations, and the reconciliation of simulation results with the actual harvested data. To this end, we hope in the third year to cap our efforts by proposing for the actual construction of IceRay-36, a 50 square-kilometer GZK neutrino detector, starting in the FY-11 season.

**Direct Labor Costs.** The University of Hawaii-Manoa (H) budget includes a full-time post-doctoral fellow, a graduate student fully devoted to the project, and two months of "casual-hire" for the PI, Professor Morse, since he is not an employee, but is "Affiliate Graduate Faculty" at UH. As such, he pays nominal fringe benefits, and normal overhead is charged on his compensation. Post-doctoral fellows at UH are supported via stipends, since they are involved in "post-doctoral training". They do not receive fringe benefits, and their stipend is not subject to overhead. Graduate students are subject to fringe benefits charges at 8.34% and normal university overhead.

The post-doc and graduate student will be responsible for the assembly, and integration of ANITA components into the IceRay detector units. Testing will include operating the units in the UH anechoic chamber and transferring the data to the Central DAQ. Analysis Software to run the Central-DAQ will be provided by our colleagues at OSU and Wisconsin. The post-doc and graduate student will also serve as daily liaisons between our IceRay collaborators as well as the IceCube experiment. The PI will work with the cognizant IceCube task leaders to ensure that IceRay works within the guidelines of "no-interference" to normal operations of the IceCube detector, and to coordinate between the various IceRay university groups, and to participate in the deployment, analysis, and modeling of IceRay.

**Travel.** Travel includes support for three to four domestic person trips per year to work with our colleagues, mostly at OSU and Madison (IceCube headquarters), and also to attend the semi-annual IceCube meetings. We also include support for two to three foreign trips to attend the annual IceCube meeting hosted by our European Collaborators, and to consult with our European IceCube collaborators that will also be analyzing the IceRay data.

**Other Direct Costs.** We include in the budget incidental materials and supplies based on our experience with similar projects.

**Equipment and Fabrication.** The IceRay array will consist of 4 remote radio-Cherenkov detector stations and a Central-DAQ data collecting station located in the IceCube Laboratory (ICL) at the South Pole. The remote stations basically consist of a suite of antennas connected to low-noise 50 kb amplifiers (LNAs), further amplified with secondary amplifiers (SSAs). Coincidences between antennas provide the local trigger and the resulting signals are time-digitized and sent back to the ICL for integration with other detectors signals and analysis. The UH is concentrating of the remote stations, while Wisconsin and OSU are constructing the ICL Central-DAQ. The detector unit cost is about 70 k\$ per station (without cables), and the detailed Central DAQ cost is about 30 K\$ to operate the four detectors. The table also includes the projected costs for the entire IceRay-36 structure.

**Indirect Costs.** F&A costs are included at the Universities negotiated rate with the cognizant agency.

### Estimated Costs for the Full IceRay.

TABLE IV: *Estimated hardware construction and deployment costs for the two arrays considered here, along with the cost basis.*

item	IceRay-36 \$K	AURA-18 \$K
Engineering design	250	250
Station costs	3000	1620
Cable costs	600	450
Drilling (3 holes/station)	...	1600
Surface deployment	600	300
Central DAQ/power system	300	300
TOTAL	4750	4520

Costs for these arrays scale according to the number of stations. In each case the common elements for the arrays are a set of order 12-16 antennas which comprise the standalone detector, receiver and digitizer blocks for each antenna, local trigger detection electronics and signal transmission electronics for an electro-optical cable. We assume that the central Data Acquisition (DAQ) system can rely on IceCube infrastructure for housing of the system and power distribution.

TABLE V: Grassroots costs for IceRay-36, along with cost basis.

<b>IceRay-36 Equipment Cost Estimate</b>				
		Rev. 2.0	GSV + PG, 09/01/2007	
		Unit Cost	TOTAL	
Detector Station	Qty.	k\$	k\$	Comment, cost basis
Upper Ground shield	1	2.0	2.0	flexible EMI mesh screen, as built costs
Antennas	16	0.75	12.0	discones (V), batwings (H), as built costs
LNA/receiver	4	7.00	28.0	Miteq LNA, ANITA rcvr design, as built costs
RF cables	16	0.05	0.8	incl. Connectors, as built costs
Power cables/connectors	6	0.20	1.2	shielded D38999 with backshells, as built
Station DAQ EMI housing	1	2.00	2.0	Machined RF-shielded encl., as built
Readout Board	1	5.00	5.0	8 layer boards, as built costs incl. labor
Trigger/FPGA	1	1.00	1.0	Virtex 4/5, RF fan-out, incl. Firmware costs
Digitizer ASIC	2	0.50	1.0	BLAB3 (TSMC 0.25um)
Trigger/discrete components	16	0.40	6.4	filters+square-laws, as built costs
Gbps transceiver	1	0.80	0.8	OKI Semiconductor, eng. Estimate
Station data cable	1	9.00	9.0	average 3km, Corning ALTOS 24 fiber,\$3/m
Station power cable	1	18.00	18.0	3km LDF-5 heliax (for EMI), \$6/m
Power Reg/misc.	1	1.20	1.2	DC-DC, housekeeping, as built costs
drilling costs, 24" holes, 50m	3	6.60	19.8	from IceCube firm drill estimate
<b>Single station costs</b>			<b>108.2</b>	<b>\$K</b>
reserves 15%			<b>16.23</b>	
<b>Total # of stations</b>	<b>36</b>			
<b>Station Subtotal</b>			<b>4479</b>	<b>\$K</b>
<b>Central DAQ</b>			<i>General Infrastructure not included--use IceCube</i>	
Gbps transceiver	60	0.80	48.0	matching links, engineering estimate
Interface Boards	10	3.50	35.0	5 stations/board, engineering estimate
cPCI DAQ crate	2	6.00	12.0	1 + spare, std. Commercial costs
cPCI CPU	2	4.00	8.0	1 + spare "
Processor farm	10	2.50	25.0	event reduction/correlation
Storage media	2	20.00	40.0	RAID systems
Network/comms	1	12.00	12.0	routers, hubs, ICL link
GPS/global clock	2	7.50	15.0	1 system + 1 spare
Power gen/regul.	1	30.00	30.0	mainframe power supply, commercial
Power pods	40	1.00	40.0	modular+spares
<b>Central DAQ Subtotal, incl 15% reserves</b>			<b>304.8</b>	<b>\$K</b>
<b>GRAND TOTAL ESTIMATE</b>			<b>4784</b>	<b>\$K</b>

For IceRay-18 we assume that 3 holes per station will be required for minimal reconstruction of vertex directions, and that the stations will have some additional complexity to accommodate the borehole geometry, including more stringent antenna construction requirements as well as embedded amplifier modules. Thus the single station costs assumed here are about \$90K for IceRay-18, and \$50K for the IceRay-36. These costs are based on pricing of a station prototype currently under development and are probably good to 15% accuracy based on current and prior vendor prices from almost all of the equipment. Cable costs are assumed to be \$10/meter based on conservative costs for a custom electro-optical cable. Drilling costs are based on estimates from other shallow holes drilled on the plateau, and assume that three holes per station will be required for effective direction reconstruction and

triggering with a single station.

Table IV give a summary estimate; more detailed costs were developed in a spreadsheet that is reproduced in Table V. The estimated base costs for the hardware and deployment here do not include scientific or professional salaries except for a single line item we include for the engineering design of the arrays. In that case we assume a single engineering man-year, estimated here at \$250K. We also do not include here the logistics costs for transport of the hardware and personnel necessary for the construction or deployment to the South Pole.

In both cases, initial estimates give hardware construction and direct deployment costs under \$5M. These systems do not require development of any new technology, thus a realistic contingency on these costs is probably well under 30%.